Land Subsidence in the Kathmandu Basin, Nepal before and after 2015 Mw 7.8 Gorkha Earthquake revealed from Time-series InSAR Analysis

PV Suresh Krishnan; Duk-jin Kim* and Jungkyo Jung

School of Earth and Environmental Sciences, Seoul National University, Seoul 151-742, Korea;

Email: krishnan92@snu.ac.kr; djkim@snu.ac.kr; ring78@snu.ac.kr

Keywords: Kathmandu Basin; Subsidence; 2015 Gorkha Earthquake; SBAS-DInSAR;

ABSTRACT

The Kathmandu Basin located in the Lesser Himalayas is composed of thick Quaternary sediments overlaying bedrocks; these sediments have experienced severe groundwater drawdown in recent years, which leads to land subsidence. In addition, the basin lies in a very tectonically active zone that was devastated by large crustal deformation from the Mw 7.8 Gorkha earthquake on April 25, 2015, measured as ~ 1 m uplift. We acquired 16 scenes of Advanced Land Observation Satellite – Phased Array L-band Synthetic Aperture Radar 1 (ALOS-PALSAR) and 20 scenes of SENTINEL-1 SAR datasets during pre- and post-seismic periods, respectively. We developed spatial and temporal velocity profiles of land subsidence in the Kathmandu Basin before and after the earthquake by applying the Small BAseline Subset – Differential Interferometric Synthetic Aperture Radar (SBAS-DInSAR) technique. The mean land subsidence rate during 2007-2010 was ~7 cm/yr in the central part of the basin, however, this rate of subsidence significantly increased to ~12 cm/yr during 2015-2016, after the Gorkha earthquake. The distribution of subsidence areas observed before and after Mw 7.8 mainshock are almost identical, indeed the subsidence rate has increased after the mainshock. These results are useful for assessing the spatiotemporal distribution of land subsidence in the Kathmandu Basin and the influence of Earthquake Environmental Effects such as large co-seismic deformation on compressible sediment layers.

1. INTRODUCTION

The Kathmandu Basin, the most densely populated valley in Nepal, is located in the middle of the Lesser Himalayas, surrounded by mountains and mainly composed of Quaternary sediments overlying bedrock. It lies in an active seismic zone that has experienced major earthquakes in the past, such as the 1934 M_s 8.2 Nepal-Bihar earthquake and a series of three large earthquakes in 1833 (Elliott et al. 2016). The M_w 7.8 Gorkha earthquake that occurred in Nepal on April 25, 2015, along the trace of MHT system (Luo and Chen 2016) is considered the second largest earthquake ever recorded in Nepal, resulting in more than 8800 casualties and widespread damage to infrastructures. According to the National Earthquake Information Center of the United States Geological Survey (USGS), the epicenter was located at Gorkha region of central Nepal at 15 km depth; the rupture propagated for about 140 km towards Kathmandu Basin. The three-dimensional surface displacements field for Mw 7.8 mainshock derived by integrated InSAR and GPS measurements (Luo and Chen 2016), shows southward horizontal deformations and gradually varied surface deformations ranging from -0.95 to 1.4 m within the radius of 120 km to the north of Kathmandu basin. The ruptures of MHT system were restricted in the subsurface and did not propagate to Main Frontal Thrust (MFT) fault. Elliott et al. (Elliott et al. 2016) confirmed this with geodetic studies as co-seismic deformation is about 0.6 m subsidence in the higher Himalaya while the Kathmandu Basin and its surrounding lesser Himalaya was uplifted about 1 m with a total horizontal movement of 2 m along south-southwest direction.

In addition to seismic activities, several studies have focused on evaluating the groundwater environment and hydrogeological characteristics of the Kathmandu Valley (Pandey and Kazama 2011, Pandey, Chapagain, and Kazama 2010). Due to urbanization, surface water resources are inadequate to meet domestic and industrial water supply demands leading to extensive groundwater extraction. However, no effort has been made to measure the actual land subsidence in the Kathmandu Basin. In this context, it is important to monitor the changes in land surface elevation for various geohazards. Land subsidence, whether due to human activities or seismic activities, can be monitored using various techniques. Conventionally, ground-based methods such as leveling and GPS (Abidin et al. 2001) were employed but these techniques are time-consuming and limited to sparse observations. Therefore, in recent years, Earth observations for several geohazards are addressed by applying the time series SAR Interferometry technique (Tomás and Li 2017). For example, to monitor spatial and temporal surface displacements (at mm/year

accuracy) caused by groundwater depletion in locations including Mexico (Sowter et al. 2016), Indonesia (Chaussard et al. 2013), the Konya Plain, and Turkey (Caló et al. 2017) as well as earthquakes such as the Gorkha (Elliott et al. 2016), and Tohoku (ElGharbawi and Tamura 2015) events.

In this study, we applied the Small Baseline Subset (SBAS) (Berardino et al. 2002) algorithm to generate time series surface displacements maps in the Kathmandu Basin before and after the 2015 Gorkha earthquake for the first time. Our main objectives is to analyse the spatial and temporal displacement pattern and rate of land subsidence in Kathmandu basin before and after earthquake using SBAS time InSAR analysis.

2. METHODOLOGY

2.1 InSAR data used

We acquired multi-temporal Synthetic Aperture Radar (SAR) Single Look Complex (SLC) images taken during pre- and post-seismic periods. For the pre-seismic phase, we acquired sixteen Fine beam single/dual (FBS/FBD) mode Phased Array L-band SAR (PALSAR) SLC images from the Advanced Land Observation Satellite-1 (ALOS-1) taken during 2007-2010 and six C-band Sentinel-1A (S1A) SLC images taken during 2014-2015. Similarly, for the post-seismic phase, we acquired twenty C-band Terrain Observation with Progressive Scans (TOPS) Interferometric wide-swath (IW) mode Sentinel-1 SLC images taken over the period of 18 months during 2015 – 2016. The characteristics and acquisition dates of these SAR datasets are listed in Table 1 and 2, respectively.

Table 1. Specifications of SAR datasets used in this study.

S.No	Description	ALOS-1	Sentinel-1
1	Acquisition mode	Stripmap	TOPS-IW
2	Wavelength (cm)	23.6	5.6
3	Incidence angle	38.72°	34.66°
4	Spatial resolution	10 m	5 x 20 m
5	Orbit repeat cycle	46 days	12 days
6	Polarization	HH	VV
7	Track	Ascending	Descending

Table 2. List of ALOS-1 PALSAR and Sentinel-1 SAR datasets used in the SBAS-DInSAR algorithm

S.No	Pre-seismic		Post-seismic
	ALOS-1	Sentinel-1A	Sentinel-1A & 1B
1	2007/01/30	2014/10/19	2015/04/29
2	2007/08/02	2014/11/12	2015/05/11
3	2007/09/17	2015/01/23	2015/05/23
4	2007/11/02	2015/02/16	2015/06/04
5	2007/12/18	2015/02/28	2015/06/16
6	2008/02/02	2015/04/17	2015/06/28
7	2008/03/19		2015/07/10
8	2008/06/19		2015/07/22
9	2008/11/04		2015/08/15
10	2008/12/20		2015/09/08
11	2009/06/22		2015/11/07
12	2009/08/07		2016/03/06
13	2009/11/07		2016/03/30
14	2009/12/23		2016/06/10
15	2010/02/07		2016/07/28
16	2010/12/26		2016/08/21
17			2016/09/14
18			2016/10/14
19			2016/11/07
20			2016/12/01

2.2 SBAS-DInSAR processing

We applied the SBAS-DInSAR technique to these data separately, in order to generate temporal profiles of land subsidence before and after the earthquake. In order to generate coherent interferograms, we chose InSAR data pairs that are having perpendicular baselines < 3000 m for ALOS-1 PALSAR and < 200 m for Sentinel-1 based on the relationship between the perpendicular and temporal baselines as shown in Figure 1. The selected ALOS-1 PALSAR InSAR data pairs are then subjected to typical Differential-InSAR (D-InSAR) (Massonnet et al. 1993) processing steps including coregistration, interferogram generation, orbital flattening, phase unwrapping and geocoding. The resampled SLC data were multi-looked with 4 x 6 looks in range and azimuth, respectively. Using SRTM 1-arcsec (30 m) DEM, the topographic phase contribution in the interferometric phase are removed to generate differential interferograms (Figure 2).

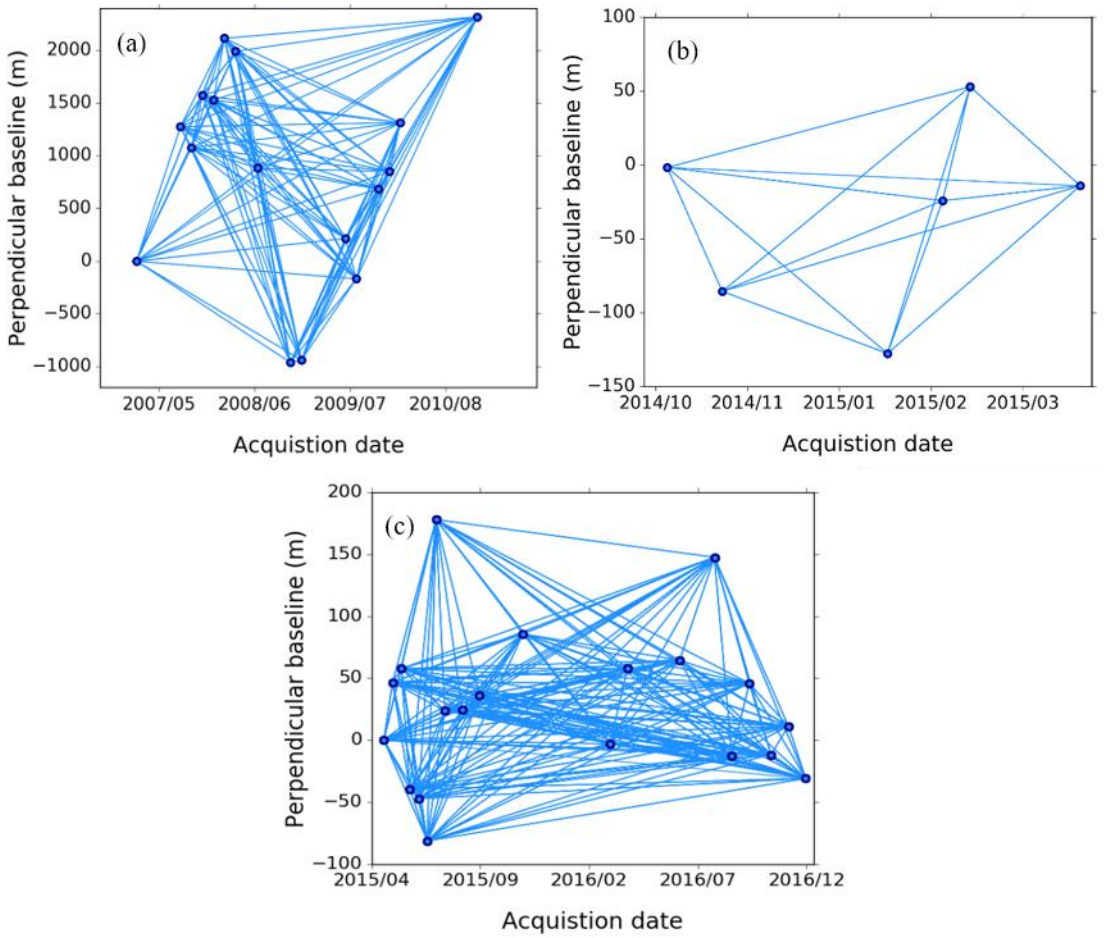

Figure 1. Perpendicular baseline vs acquisition dates for (**a**) ALOS-1 PALSAR during 2007-2010 (pre-seismic) (**b**) Sentinel-1 during 2014-2015 (pre-seismic) and (**c**) Sentinel-1 during 2015-2016 (post-seismic)

Whereas the acquisition of Sentinel-1 is different from the conventional method, the coregisration of Sentinel-1 IW TOPS mode InSAR data requires extremely precise coregistration (Dai et al. 2016). This can be achieved through geometric coregistration using precise orbits and DEM followed by estimation of individual misregistration errors with enhanced spectral diversity (Fattahi, Agram, and Simons 2016). The methodology for interferometric processing of S1A TOPS mode data applied in this study is described in (Yagüe-Martínez et al. 2016). The interferograms are computed with multi looks of 10 x 2 in range and azimuth, respectively along with precise orbits provided by European Space Agency (ESA). In the SBAS time series algorithm, residual orbital ramps were estimated in each pair and removed individually and by the network. Finally, the two time-series surface displacements with spatial resolutions of about 40 x 20 m^2 and 50 x 40 m^2 for ALOS-1 PALSAR and Sentinel-1, respectively were derived for each coherent pixel > 0.3 by SBAS inversion of unwrapped interferograms (Figure 3).

3. RESULTS & DISCUSSION

Figure 3 shows the spatio-temporal displacement maps derived from SBAS-DInSAR analysis using ALOS-1 PALSAR data obtained during 2007 – 2010 (4 years). Since the Kathmandu Basin is predominantly a mountainous region with an urban area in the center, we subsetted the urban area based on the mean coherence value (> 0.3) in order to provide reliable time series results. Overall, the significant subsidence is observed in the central part of the Kathmandu, where no such strong subsidence has reported in the previous studies. We identified three locally subsiding regions in the basin: Lazimpet, Kalimati, and Patan (hereafter, referred as zone 1, 2 and 3, respectively).

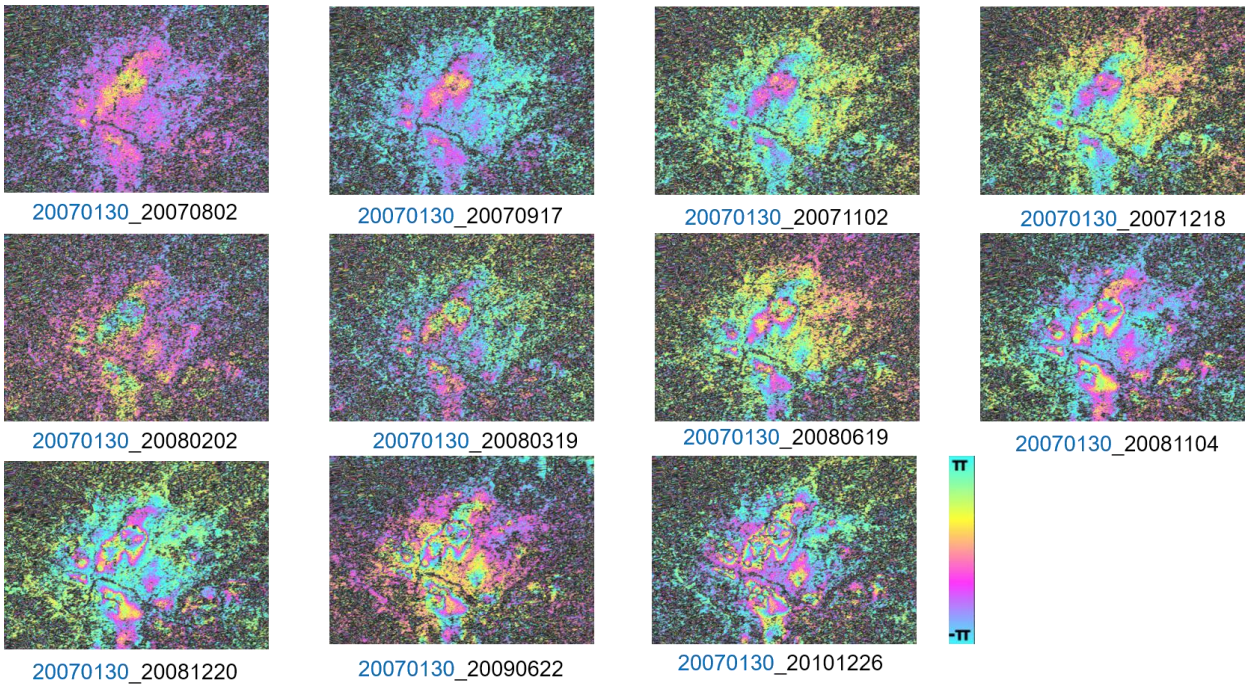

Figure 2. Differential phase measurements measured between each SAR pair acquired by ALOS-1 PALSAR data during 2007-2010

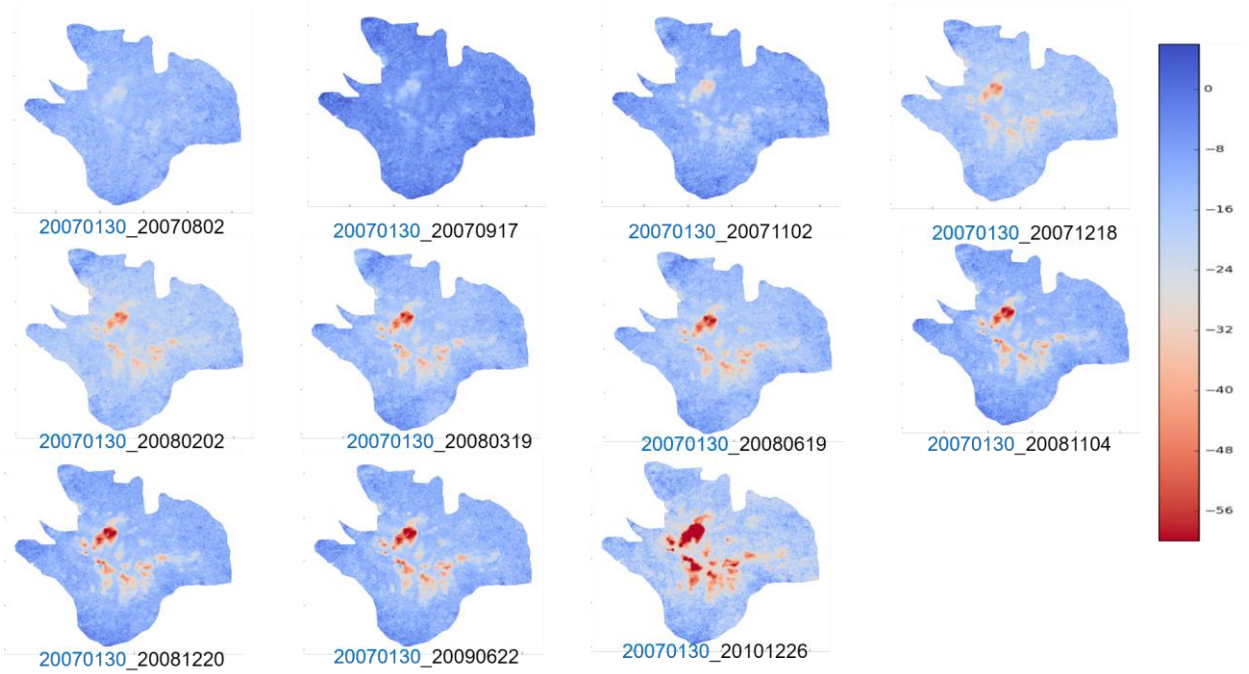

Figure 3. shows the spatio-temporal displacement maps derived from SBAS-DInSAR analysis using ALOS-1 PALSAR data obtained during 2007 – 2010 (4 years).

Figures 4a & b show the pre-seismic surface displacements in the Kathmandu Basin measured by ALOS-PALSAR and Sentinel-1A data. During the pre-seismic phase, the surface displacement is varied from 14cm to -53cm where the maximum relative subsidence was observed as -53 cm from ALOS PALSAR datasets acquired over 4 years (2007-2010) and -8 cm from 6 Sentinel-1A datasets acquired over 6 months (2014-2015) in the LOS direction. Figure 4c shows the post-seismic cumulative surface displacements, measured 2015-2016. The estimated maximum LOS displacement is -25 cm in Zone 1, -13 cm in Zone 2 and -11 cm in Zone 3. It can be clearly seen that the subsidence in the central basin is expanding for more than 10 years, approximately. Besides the subsidence accumulation in Zones 1, 2 and 3 in the basin, other regions are observed to be stable or with minimum surface displacements (less than 2cm/yr).

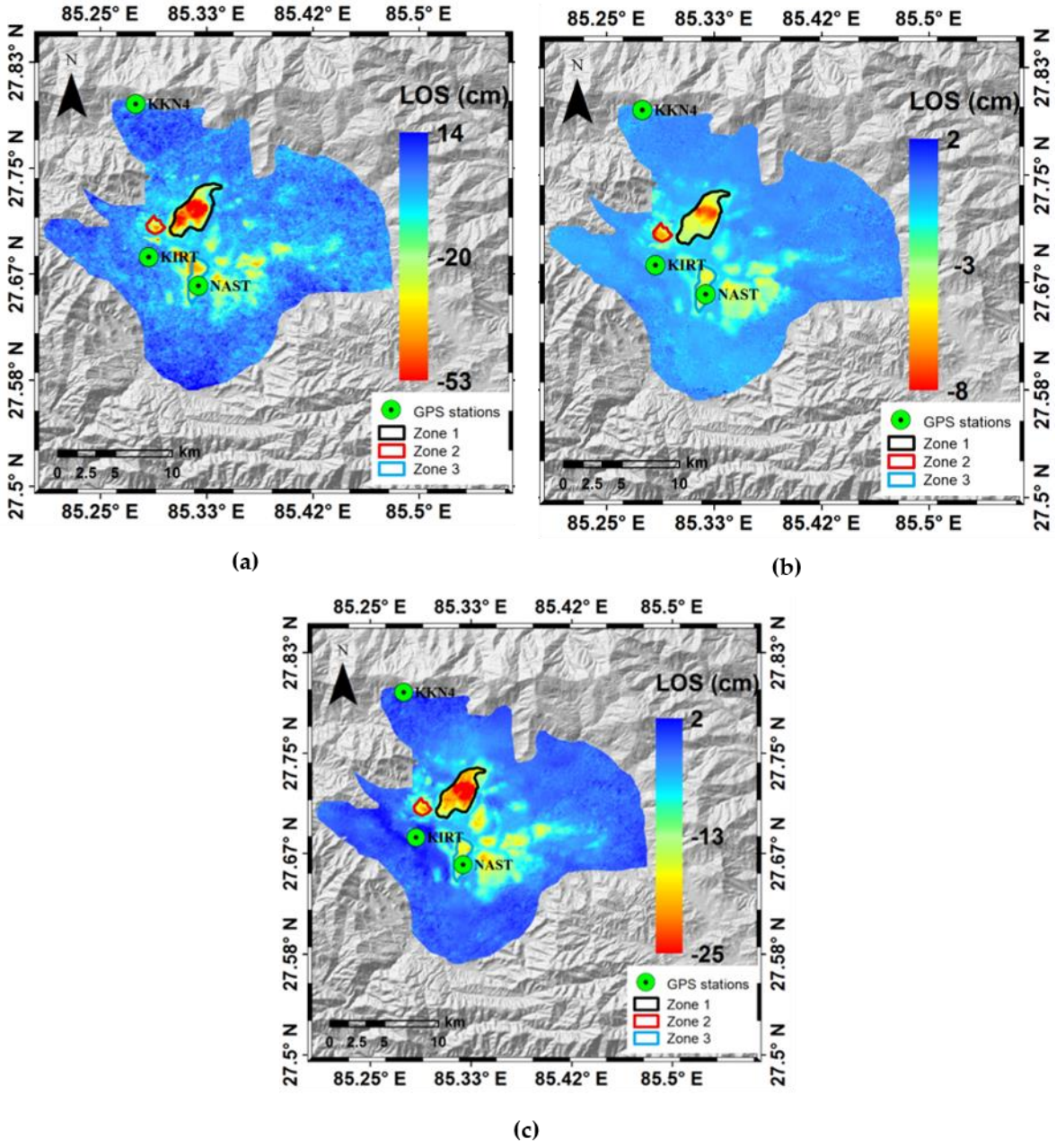

Figure 4. Cumulative LOS InSAR displacements map from SBAS-DInSAR analysis superimposed on a DEM (**a**) pre-seismic displacement measured from ALOS-1 (2007-2010) (**b**) pre-seismic displacement measured from Sentinel-1 (2014-2015) and (**c**) post-seismic displacement measured from Sentinel-1 (2015-2016). Colorbars shows relative displacement where blue (positive) represents uplift and red (negative) shows subsidence.

4. CONCLUSIONS

In this study, we investigated land subsidence in the Kathmandu Basin before and after the 2015 Gorkha earthquake by using the SBAS-DInSAR time series algorithm with satellite derived ALOS-1 PALSAR and Sentinel-

1A TOPS mode SAR data. ALOS-1 SBAS-DInSAR time series results from 2007-2010 report a cumulative absolute land subsidence of about 60cm in the Kathmandu Basin with a maximum rate of 15 cm/yr and a mean velocity of about 7 ± 0.1 cm/yr in Zones 1, 2 and 3. Sentinel-1 SBAS-DInSAR time series (2015-2016) implied that the post-seismic subsidence velocity in highly compressible clay layers (Zones 1, 2 and 3) increased significantly to 12 ± 0.1 cm/yr following the large co-seismic crustal deformation caused by 2015 gorkha earthquake. Our findings demonstrate the importance of monitoring spatiotemporal surface displacements in seismically active areas in response to anthropogenic subsidence and the effects of major earthquakes on the Kathmandu sedimentary basin.

ACKNOWLEDGEMENT

This research is supported in part by a grant (16RDRP-B076564-03) from the Regional Development Research Program funded by the Ministry of Land, Infrastructure and Transport of the Korean government, and in part by the Korea Research Foundation under Project (2016M1A3A3A04936872). ALOS PALSAR data used in this study are provided by JAXA as a part of Research Agreement (PI No.1407). Sentinel-1 data used in this study are provided by ESA through the Sentinel-1 Scientific Data Hub.

REFERENCES

Abidin, Hasanuddin Z., Rochman Djaja, Dudy Darmawan, Samsul Hadi, Arifin Akbar, H. Rajiyowiryono, Y. Sudibyo, I. Meilano, M. A. Kasuma, J. Kahar, and Cecep Subarya. 2001. "Land Subsidence of Jakarta (Indonesia) and its Geodetic Monitoring System." *Natural Hazards* 23 (2):365-387. doi: 10.1023/a:1011144602064.

Berardino, Paolo, Gianfranco Fornaro, Riccardo Lanari, and Eugenio Sansosti. 2002. "A new algorithm for surface deformation monitoring based on small baseline differential SAR interferograms." *IEEE Transactions on Geoscience and Remote Sensing* 40 (11):2375-2383.

Caló, Fabiana, Davide Notti, Jorge Galve, Saygin Abdikan, Tolga Görüm, Antonio Pepe, and Füsun Balik Şanli. 2017. "DInSAR-Based Detection of Land Subsidence and Correlation with Groundwater Depletion in Konya Plain, Turkey." *Remote Sensing* 9 (1):83.

Chaussard, Estelle, Falk Amelung, Hasanudin Abidin, and Sang-Hoon Hong. 2013. "Sinking cities in Indonesia: ALOS PALSAR detects rapid subsidence due to groundwater and gas extraction." *Remote Sensing of Environment* 128:150-161. doi: http://dx.doi.org/10.1016/j.rse.2012.10.015.

Dai, Keren, Zhenhong Li, Roberto Tomás, Guoxiang Liu, Bing Yu, Xiaowen Wang, Haiqin Cheng, Jiajun Chen, and Julia Stockamp. 2016. "Monitoring activity at the Daguangbao mega-landslide (China) using Sentinel-1 TOPS time series interferometry." *Remote Sensing of Environment* 186:501-513. doi: http://dx.doi.org/10.1016/j.rse.2016.09.009.

ElGharbawi, Tamer, and Masayuki Tamura. 2015. "Coseismic and postseismic deformation estimation of the 2011 Tohoku earthquake in Kanto Region, Japan, using InSAR time series analysis and GPS." *Remote Sensing of Environment* 168:374-387.

Elliott, JR, R Jolivet, PJ González, J-P Avouac, J Hollingsworth, MP Searle, and VL Stevens. 2016. "Himalayan megathrust geometry and relation to topography revealed by the Gorkha earthquake." *Nature Geoscience*.

Fattahi, Heresh, Piyush Agram, and Mark Simons. 2016. "A Network-Based Enhanced Spectral Diversity Approach for TOPS Time-Series Analysis." *IEEE Transactions on Geoscience and Remote Sensing*.

Luo, Haipeng, and Ting Chen. 2016. "Three-Dimensional Surface Displacement Field Associated with the 25 April 2015 Gorkha, Nepal, Earthquake: Solution from Integrated InSAR and GPS Measurements with an Extended SISTEM Approach." *Remote Sensing* 8 (7):559.

Massonnet, Didier, Marc Rossi, Cesar Carmona, Frederic Adragna, Gilles Peltzer, Kurt Feigl, and Thierry Rabaute. 1993. "The displacement field of the Landers earthquake mapped by radar interferometry." *Nature* 364 (6433):138-142.

Pandey, Vishnu Prasad, Saroj Kumar Chapagain, and Futaba Kazama. 2010. "Evaluation of groundwater environment of Kathmandu Valley." *Environmental Earth Sciences* 60 (6):1329-1342. doi: 10.1007/s12665-009-0263-6.

Pandey, Vishnu Prasad, and Futaba Kazama. 2011. "Hydrogeologic characteristics of groundwater aquifers in Kathmandu Valley, Nepal." *Environmental Earth Sciences* 62 (8):1723-1732. doi: 10.1007/s12665-010-0667-3.

Sowter, Andrew, Moh Bin Che Amat, Francesca Cigna, Stuart Marsh, Ahmed Athab, and Lubna Alshammari. 2016. "Mexico City land subsidence in 2014–2015 with Sentinel-1 IW TOPS: Results using the Intermittent SBAS (ISBAS) technique." *International Journal of Applied Earth Observation and Geoinformation* 52:230-242.

Tomás, Roberto, and Zhenhong Li. 2017. Earth observations for geohazards: Present and future challenges. Multidisciplinary Digital Publishing Institute.

Yagüe-Martínez, N., P. Prats-Iraola, F. Rodríguez González, R. Brcic, R. Shau, D. Geudtner, M. Eineder, and R. Bamler. 2016. "Interferometric Processing of Sentinel-1 TOPS Data." *IEEE Transactions on Geoscience and Remote Sensing* 54 (4):2220-2234. doi: 10.1109/TGRS.2015.2497902.